GMR
The Original

EFFECT OF ULTRA-DILUTED BERBERIS VULGARIS ON NF-KB GENE EXPRESSION AND P38 MAPK PROTEIN SIGNALLING IN RAT RENAL TISSUE: A COMBINED QRT-PCR AND WESTERN BLOT STUDY

J. Sundareshan[1*], Winston Vargeese[2]

[1]Department of Human Anatomy, Dr Hahnemann Homoeopathy Medical College and Research Centre, Rasipuram, Namakkal District, Tamil Nadu, India
[2]Department of Homoeopathic Materia Medica, Sarada Krishna Homoeopathic Medical College, Kulasekharam, Kanyakumari District, Tamil Nadu, India
Corresponding author: Dr J. Sundareshan, Email: sakthisundar.87@gmail.com. ORCID: 0009-0002-7114-5525

ABSTRACT

Background: Nuclear factor-κB and p38 mitogen- activated kinase are inflammatory and cellular stress response signalling which contributes the renal inflammation. Berberis vulgaris has the principal alkaloid called berberine, which has been found to be anti-inflammatory and antioxidant in many studies, but the effect of preparations of ultra-highly diluted form on these pathways has not been discovered.

Objective: To evaluate NF-κB gene expression and p38 MAPK protein expression in rat renal tissue in an ethylene glycol-induced nephrolithiasis model, across nine experimental groups (G1–G9), following treatment with ultra-diluted Berberis vulgaris 30CH (10^{-60}), 200CH (10^{-400}, 1M (10^{-2000}), 10M (10^{-20000}), 0/1 LM

Methods: This study was carried out using ethylene glycol-induced nephrolithiasis in male Wistar rats;
Fifty-four male Wistar rats were selected and divided into nine groups; six rats (n=6). Groups were labelled as follows: G1(normal control), G2 as disease control (ethylene glycol only), G3, G4, G5, G6 and G7 as preventive groups with five ultra-diluted Berberis Vulgaris, G8 as a Therapeutic group and G9 as Standard drug control (Cystone). NF-κB transcripts were quantified by SYBR-Green qRT-PCR (QuantStudio 5) with GAPDH as a reference, using the $2^{-\Delta\Delta Ct}$ method. RNA was extracted by the TRIzol method, DNase-treated, and reverse transcribed. Total p38 MAPK protein was assessed using SDS-PAGE/western blot, and band intensity was quantified using ImageJ after normalising to β-actin. Data are expressed as mean ± SD and compared by one-way ANOVA; $p < 0.05$ was considered significant. Before statistical analysis, normality for each experimental group was tested using the Shapiro–Wilk test. All groups showed a normal distribution ($p > 0.05$), indicating that the assumption of normality was met. Homogeneity of variances was subsequently evaluated using Levene's test, confirming equal variances among groups ($p > 0.05$). Therefore, one-way analysis of variance **(ANOVA)** was performed, followed by Tukey's multiple comparisons test for pairwise group comparisons. Statistical analyses were conducted using SPSS SOFTWARE (Version 2026), and a two-tailed **$p < 0.05$** was considered statistically significant.

Results: One-way ANOVA showed a highly significant difference in p38 MAPK protein expression among the nine groups ($F(8,45) = 264.77$, $p < 0.0001$) and in NF-κB gene expression ($F(8,45) = 3.73$, $p = 0.00203$). The disease control (G2) showed the highest NF-κB (RQ = 2.323) and p38 MAPK (33.8 ± 1.4%) expression, consistent with activation of inflammatory signalling by ethylene glycol. Treatment groups showed reduced expression of both markers relative to disease control, with the greatest suppression in G6 (10M: NF-κB RQ = 0.097; p38 MAPK = 18.1 ± 0.7%) and G3 (30CH: RQ = 0.026; p38 MAPK = 17.2 ± 2.1%). The values of both the inflammatory markers NF-κB and p38 MAPK are strongly expressed and correlated among the groups (Pearson $r = 0.88$, $p = 0.0016$).

Conclusion: Ultra-diluted Berberis vulgaris shows modulatory changes in the inflammatory pathway, NF-κB transcription and p38 MAPK protein expression in renal tissue. Because ultra-dilutions beyond the Avogadro limit contain no molecules of the source substance, this association should be interpreted as control-referenced and hypothesis-generating; independent replication with a successed-vehicle comparator is warranted before mechanistic or therapeutic claims are drawn.

KEYWORDS: NF-κB; p38 MAPK; qRT-PCR; Western blotting; Berberis vulgaris; berberine; renal inflammation; Wistar rat; ethylene glycol nephrolithiasis; high dilutions.

INTRODUCTION

Our body's primary tissue response for defence and repair is inflammation, which triggers a similar reaction in renal tissues. Numerous studies demonstrate that the two main signalling pathways frequently mentioned are Nuclear factor kappa B (NF-kB), a master transcription factor that regulates inflammatory mediators such as cytokines and chemokines. Persistent elevation of these inflammatory pathways leads to renal diseases [1-4].

The other parallel pathway of inflammatory reaction by oxidative stress is the p38 mitogen-activated protein kinase (p38 MAPK) [5–8]. NF-κB and p38 MAPK are functionally interconnected, so this is a representative transcription factor and a representative kinase that provides a fuller picture of inflammatory tone in renal tissue than either marker alone [9].

The p38 mitogen-activated protein kinase (p38 MAPK) pathway acts in parallel, transducing inflammatory, oxidative and stress stimuli into cytokine production and inflammatory gene transcription. NF-κB and p38 MAPK are functionally interconnected, so co-measurement of a representative transcript and a representative kinase provides a fuller picture of inflammatory tone in renal tissue than either marker alone [9].
Ethylene glycol induces biochemical and molecular changes in renal tissues by producing reactive oxygen species and activating the NF-kB and p38 mitogen-activated protein kinase. The inflammation produces the aggregation of calcium oxalate crystals in the renal tubules. The crystals are produced by hepatic oxidation of ethylene glycol via alcohol and aldehyde dehydrogenases, which produces glycolic acid, driving severe anion-gap metabolic acidosis, and oxalic acid, leading to hyperoxaluria, which causes mitochondrial damage and influences the above inflammatory signalling pathways.
In ultra-dilutions, beyond the Avogadro limit, molecules of the source substance are traced, but nanoparticle persistence and physicochemical changes can be attributed to the controls with an appropriate disease model, blinding and replication. This study shows the changes in NF-κB by qRT-PCR and p38 MAPK protein by western blot analysis across nine groups by inducing an ethylene glycol nephrolithiasis model, treated with different ultra-high dilutions of Berberis vulgaris in the rat renal tissues.

Aim and objectives

We aim to study the effects of ultra-high dilutions of Berberis vulgaris (30 CH (10^{-60}), 200CH (10^{-400}), 1M (10^{-2000}), 10M (10^{-20000}), and 0/1 LM) on the NF-kB genes and p38MAPK proteins in male Wistar rats with induced nephrolithiasis caused by ethylene glycol. This also finds that these dilutions can change the important signalling pathways related to inflammation and cellular stress compared to molecular effects in healthy, diseased and standard treatment controls.

Pathophysiology of renal tissue injury and NF-kB pathway activation in ethylene glycol toxicity:

Ethylene glycol induces hepatic biochemical changes in tubulointerstitial inflammation ranging from moderate to severe. The pathophysiology of lithiasis in the ethylene glycol model in rats and humans is the same, producing calcium oxalate crystals. The crystals are produced by hepatic oxidation of ethylene glycol via alcohol and aldehyde dehydrogenases, which produces glycolic acid, driving severe anion-gap metabolic acidosis, and oxalic acid, leading to hyperoxaluria [24][25][26][27]. This oxalic acid binds with the luminal calcium ions and forms insoluble calcium oxalate crystals. So, the aggregation of the crystals causes mitochondrial damage to produce a robust inflammatory cascade driven by the Nuclear Factor kappa B (NF-κB) pathway and p38 MAPK (Mitogen-Activated Protein Kinase). This damages renal cells and leads to crystal aggregation by triggering reactive oxygen species. Free NF-kB translocate to the nucleus, upregulating pro-inflammatory chemokines and cytokines. This drives extracellular matrix deposition, tubular atrophy, and irreversible renal fibrosis [28][29].

MATERIALS AND METHODS

Study design and animals

For this experiment, male Wistar rats were used between the ages of 6-8 weeks, weighing approximately 150-230 g. A total of 54 rats were housed at a temperature of about 24-26c maintaining the 12-hr light and 12 hr dark cycle. With free access to a commercial diet and water ad libitum. 54 rats were randomly allocated into nine groups(G1-G9), each group having 6 animals (n=6). Samples collected at the end of the experiment for biological assay were coded using a blinding method until completion of the analysis.

Randomisation: All 54 animals were grouped into 9 (G1 to G9) experimental groups, each group having 6 (n=6) animals coded for each group, and animals in each group were allocated using computer-generated simple randomised codes. Randomisation allocation was performed before the administration of ethylene glycol by an investigator not involved in treatment or outcome assessment to ensure allocation and minimise bias.

Sample size justification: according to the CPCSEA recommendations, a sample size of 6 (n=6) animals per group was selected based on previous ethylene glycol-induced models for detecting biologically meaningful differences, according to the principle of reduction under the 3Rs

Animal attrition: All 54 rats completed the study having no attrition during the study period that included in the final statistical analysis.

Group allocation and intervention

Group	n	Treatment administered	Duration	Purpose
G I	6	Normal saline (0.9%) drinking water	60 days	Normal control
G II	6	0.75% ethylene glycol in drinking water	60 days	Disease control (nephrolithiasis)

Group	n	Treatment administered	Duration	Purpose
G III	6	0.75% EG + Berberis vulgaris 30CH, one drop TDS orally in 0.9% saline	60 days	Preventive – 30CH
G IV	6	0.75% EG + Berberis vulgaris 200CH, one drop TDS	60 days	Preventive – 200CH
G V	6	0.75% EG + Berberis vulgaris 1M, one drop TDS	60 days	Preventive – 1M
G VI	6	0.75% EG + Berberis vulgaris 10M, one drop TDS	60 days	Preventive – 10M
G VII	6	0.75% EG + Berberis vulgaris 0/1 LM, one drop TDS	60 days	Preventive – LM potency
G VIII	6	0.75% EG (Day 0–28); Berberis vulgaris 200CH from Day 14–60, one drop TDS	60 days	Therapeutic (post-induction)
G IX	6	0.75% EG + Cystone 750 mg/kg body weight, orally	60 days	Standard-drug control

Table 1. Group allocation, dosing, experiment schedule and purpose of study (N = 54; n = 6 per group).

Preparation of the test substance

The test substance for the study was sourced from Dr Willmar Schwabe India Pvt Ltd: ultra-diluted Berberis vulgaris, potencies for 30CH (batch no: 1129002), 200CH (1128660), 1M (batch n0:1127631), 10M(LDD- batch no HD21/455), 0/1 LM are taken; each potency is prepared as an orally administered substance by adding one drop of dilution from each potency into each 30 ml dropper container with 0.9% normal saline. This is to be administered for 60 days for the groups G3, G4, G5, G6, G7, G8, labelled as preventive and therapeutic groups. G1 was administered with unsuccussed 0.9% saline, G2 was administered with ethylene glycol alone for 60 days, marked as the disease baseline, and G9 was administered with the standard drug control cystone for 60 days.

Tissue collection

After completion of the 60-day experimental period, animals were handled in accordance with CPCSEA guidelines under the approved protocol. Each rat was deeply anaesthetised by intraperitoneal injection of ketamine (80 mg/kg) and xylazine (10 mg/kg), and, following complete loss of the pedal reflex, was humanely euthanised by exsanguination to clear blood from the organs [13,14]. A midline abdominal incision was made using sterile instruments, and both kidneys were dissected free, excised and rinsed in ice-cold normal saline to remove residual blood. One portion of each kidney was snap-frozen in liquid nitrogen and stored at −80 °C for qRT-PCR and Western blot analysis; a second portion was fixed in 10% neutral buffered formalin for histopathology. The CPCSEA principles of Replacement, Reduction and Refinement were followed throughout.

RNA isolation, DNase treatment and cDNA synthesis

Total RNA was isolated using the TRIzol method according to the manufacturer's instructions. Tissue pellets were centrifuged in DEPC-treated tubes at 5000 rpm for 10 min, and 700 µL TRIzol was added per 1×10^7 cells for lysis. Following the addition of 300 µL chloroform and vigorous mixing, the aqueous phase was separated by centrifugation (12,000 rpm, 20 min, 4 °C), and RNA was precipitated with 700 µL isopropanol, pelleted (12,000 rpm, 20 min, 4 °C), washed with 70% ethanol, air-dried and resuspended in 30 µL nuclease-free water. RNA quantity and quality were assessed by UV-Vis spectrophotometry and 1% agarose gel electrophoresis.

Quantitative real-time PCR

Approximately 1.5 µg of total RNA was reverse-transcribed using MMLV reverse transcriptase with oligo(dT) priming (42 °C, 60 min; 70 °C, 5 min; hold at 4 °C). qRT-PCR was performed using the PowerUp SYBR Green kit (Applied Biosystems) on a QuantStudio 5 system (Applied Biosystems), following minimum-information reporting principles for quantitative PCR experiments [15]. NF-κB expression was quantified by the relative quantification ($2^{-\Delta\Delta Ct}$) method [16], normalised to GAPDH as the endogenous control, with the normal control group (G1) as calibrator. Primer sequences are given in Table 2.

Gene	Direction	Sequence (5′→3′)
NF-κB	Forward	GCAAACCTGGGAATACTTCATGTGACTAAG
NF-κB	Reverse	ATAGGCAAGGTCAGAATGCACCAGAAGTCC
GAPDH	Forward	GGGTGATGCTGGTGCTGAGTATGT
GAPDH	Reverse	AAGAATGGGAGTTGCTGTTGAAGTC

Table 2. Primer sequences used for qRT-PCR.

Western blot analysis

Equal amounts of protein (50–100 µg) were separated by SDS-PAGE on a 10% discontinuous polyacrylamide gel using a standard glycine buffer system [17] and electrotransferred onto PVDF membranes [18]. Membranes were blocked with 5% non-fat dry milk in TBST for 1 hour at room temperature and incubated overnight at 4 °C with rabbit monoclonal anti-total-p38 MAPK antibody [19] (Cell Signalling Technology, Cat. No. 8690; 1:1000). After washing, membranes were incubated with HRP-conjugated goat anti-rabbit IgG (Cell Signalling

Technology, Cat. No. 7074; 1:5000) for 1 hour at room temperature. Membranes were reprobed with mouse monoclonal anti-β-actin antibody (Sigma-Aldrich, clone AC-15, Cat. No. A5441; 1:5000) followed by HRP-conjugated goat anti-mouse IgG (Cell Signalling Technology, Cat. No. 7076; 1:5000).
Western blot was run for each experimental group to validate the target expression pattern, with the primary antibody (cat No: 8690), representing the total P38 MAPK protein expression. Protein bands were seen using DAB substrate, and densitometry analysis was performed in ImageJ with consistent Western blot principles.

Densitometry

Each p38 MAPK band was measured in ImageJ with the corresponding β-actin loading-control band from the same lane. Relative expression values are normalised to the mean of the control group, which is assigned as 100%, using the following formula,

Relative expression (% of control) = (normalised intensity of sample ÷ mean normalised intensity of control group) × 100

Statistical analysis

Normality was tested for each group using the Shapiro-Wilk test; normal distribution for all groups ($p>0.05$), meeting the assumption of normality. Homogeneity of variance was evaluated using Levene's test for equal variance among the groups ($p>0.05$). One-way analysis of variance (ANOVA) was performed for the comparison of pairwise comparison of groups. Data were presented as mean ± SD (n = 6 per group). Statistical analyses were conducted using SPSS statistical software (Version 2026), and a two-tailed **$p < 0.05$** was considered statistically significant.

RESULTS

p38 MAPK protein expression

Immunoreactive bands (p38kDa) were detected in all the groups. One-way ANOVA showed a highly significant difference in p38 MAPK protein expression among all nine groups ($F(8.45) = 264.77$, $p<0.0001$),

Table 4. Disease control G2 expresses the highest 35.12%, G9, 28.4%, and the lowest in G3, G6, 16.16%, 18.18%.

Group	Band area (a.u.)	Relative expression (%)
G1	8562.12	24.15
G2	13005.37	35.12
G3	6346.47	16.16
G4	7158.24	19.97
G5	7915.23	22.56
G6	6626.98	18.18
G7	7593.98	21.03
G8	8765.10	26.45
G9	9301.34	28.04

Table 3. Densitometric analysis of p38 MAPK expression by group.

Source	DF	Sum of squares	Mean square	F	P-value
Groups (between)	8	1343.3712	167.9214	264.7693	<0.0001
Error (within)	45	28.5398	0.6342		
Total	53	1371.911			

Table 4. One-way ANOVA summary for p38 MAPK protein expression across groups.

p38 MAPK expression was markedly upregulated in G2 and downregulated in G3 and G7 relative to the normal control (G1), while G4–G6 and G8–G9 maintained stable, moderate expression. Consistent β-actin levels across all lanes confirmed equal protein loading.

An indicative post hoc comparison was derived from the group means (Table 3) and the pooled mean square error reported in Table 4, using Tukey's HSD = $q(\alpha, k, df) \times \sqrt{(MSE/n)}$, which gives HSD ≈ 1.46 ($\alpha = 0.05$, $k = 9$, $df = 45$). On this basis, G2 differed significantly from every other group, and G1 differed significantly from G3, G4, G6, G7, G8 and G9. The statistical summary confirmed the output from GraphPad Prism with the raw per-animal data. In that G3 differs from G6, G8, and G9, G5 Vs G7 is borderline, and G4 Vs G7 did not reach significance.

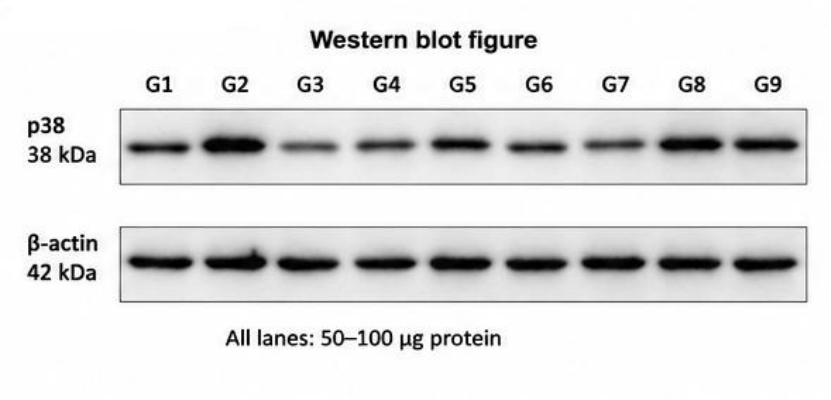

Figure 2 — Molecular weight markers labelled, showing the p38 MAPK and β-actin loading-control bands for G1–G9 for western blotting.

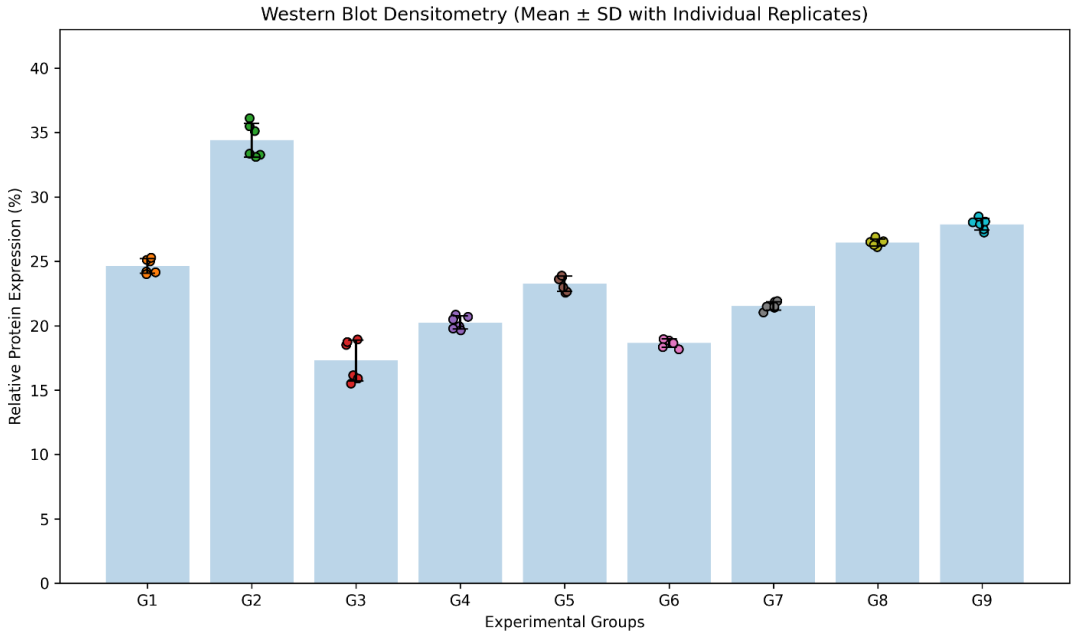

Figure 3: Densitometric expression for p38 MAPK through western blotting shows highest expression in the G2 disease control group; treatment groups, particularly G3 and G6, show significantly reduced expression, suggesting an anti- inflammatory effect. Bars represent mean ± SD, and dots represent individual biological replicates (n = 6).

NF-κB gene expression

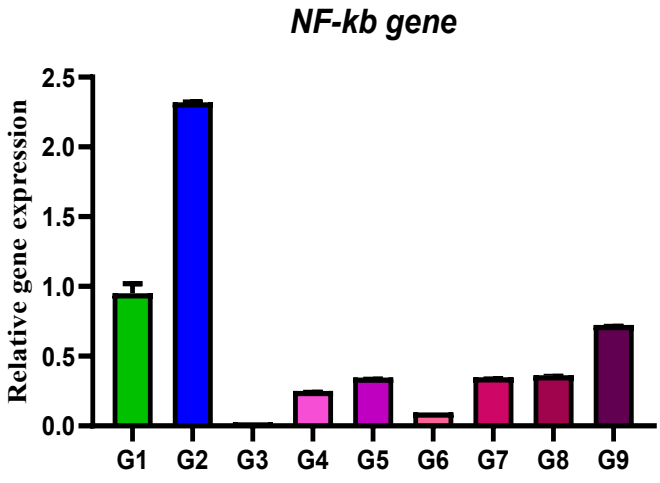

Figure 4 shows the NF-KB gene expression; the disease control group showed a marked increase (2.3- fold) compared with the normal control (0.95- fold). Results confirming activation of inflammatory pathways following ethylene administration.NF-Kb expression was observed greatest in G3 & G6, followed by G4, G5, G7 AND G8. Whereas G9 showed moderate inhibition.

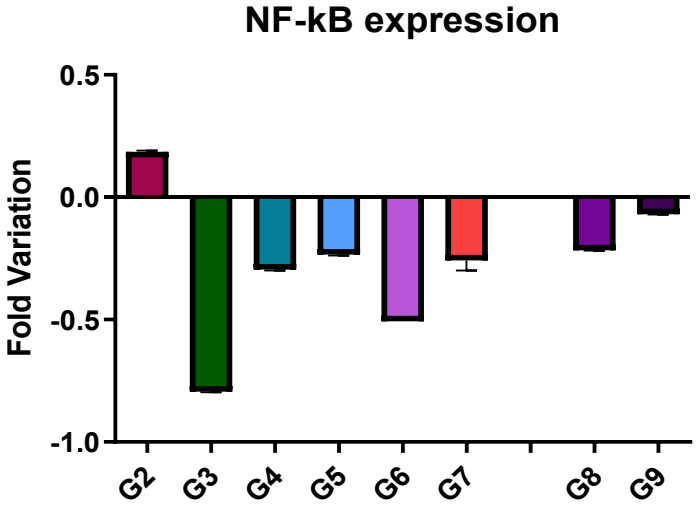

Figure 5 Demonstrates the fold variation of negative values for all treated groups relative to the disease control. Findings show consistent downregulation of the treatment, effectively suppressing the NF-kB mediated inflammatory signalling and contributing to the nephroprotective activity.

The amplification for the targeted genes for NF-κB and GAPDH from the qRT-PCR analysis generated expected amplification products of approximately 128bp to 143 bp, respectively. Each primer shows a well-defined melting curve, indicating specific amplification without detectable primer-dimer formation.

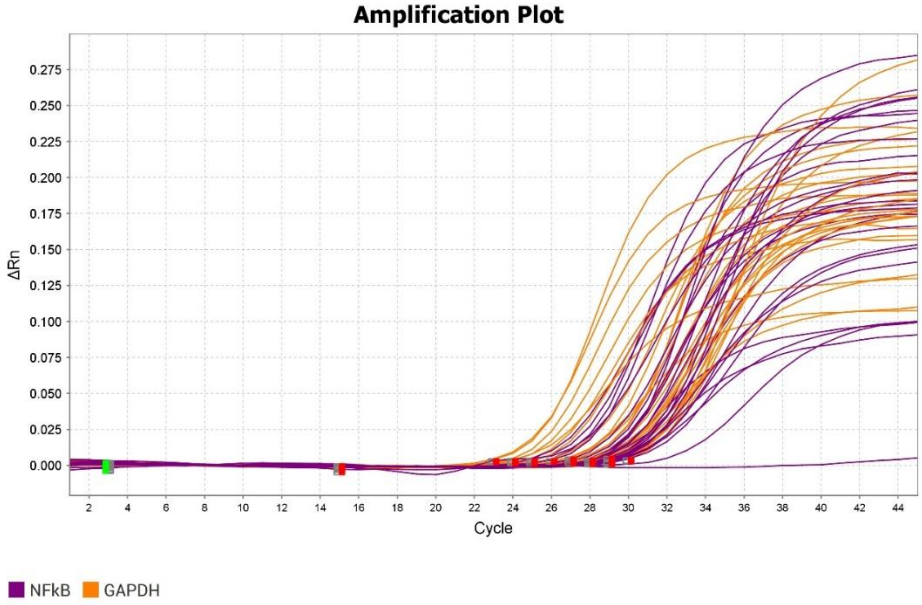

Figure:1- standard curve for serial dilution points to the effective values of amplification for GAPDH and NF-κB

One-way ANOVA showed a statistically significant difference in NF-κB expression among the nine groups ($F(8,45) = 3.7275$, $p = 0.00203$; Table 5). Among all the groups, G2 disease control (RQ= 2.323) shows a marked increase in gene expression, G3 (30CH, RQ=0.026) and G6 (10M, RQ= 0.097) greatest suppression followed by G4 (200 CH, RQ=0.253), G5 (1M, RQ= 0.392), G7 (0/1 LM, RQ= 0.349) and G8 (therapeutic 200 CH, RQ= 0.367), G9 (cystone, RQ= 0.626) showed lowest reduction among treated groups. The overall expression for the NK-KB pathway shows downregulation in the treatment group, and it shows more in G3 and G6.

Source	DF	Sum of squares	Mean square	F	P-value
Groups (between)	8	63.2494	7.9062	3.7275	0.00203
Error (within)	45	95.4455	2.1210		
Total	53	158.6949	2.9942		

Table 5: Summary of one-way ANOVA among the groups for NF-kB expression.

Two pairwise differences were statistically significant by Tukey's multiple comparisons test, in that G2 Vs G2 and G2 Vs G4 were (p=0.0042) and (p=0.0023). other pair wise comparison among the groups with G2 comparison did not reach $p > 0.05$ at this sample size

Tukey's multiple-comparisons test identified two statistically significant pairwise differences: G2 versus G3 ($p = 0.0042$) and G2 versus G4 ($p = 0.0023$). All other pairwise comparisons, including G2 versus the remaining treated groups, did not reach significance ($p > 0.05$) at this sample size. The omnibus ANOVA establishes an overall group difference; a complete pairwise comparison table for every group pair, once finalised from the primary statistical output, would strengthen this section and is recommended for the supplementary material.

An algebraic back-calculation of Tukey's HSD from the pooled mean square error in Table 5 ($HSD \approx 2.68$ at $\alpha = 0.05$) does not reproduce the two significant comparisons reported above, since the G2 vs. G3 and G2 vs. G4 mean differences (2.30 and 2.07, respectively) both fall below this threshold. This discrepancy suggests that the original post hoc analysis may have applied Dunnett's test against the single disease-control comparator (which carries a smaller critical value than an all-pairs Tukey test) rather than a full pairwise Tukey comparison, or that individual group variances depart from the pooled estimate. We recommend confirming which post hoc procedure was actually applied in GraphPad Prism, and reporting the complete comparison table — each treated group versus G2 and versus G1, with exact p-values — as a supplementary table, since an algebraic approximation from summary statistics cannot substitute for software output computed on the original per-animal dataset.

Relationship between NF-κB and p38 MAPK expression

Summary of Table 6 represents the NF-κB and p38 MAPK expression across the nine groups; values of both are strongly and positively correlated (Pearson $r = 0.88$, $p = 0.0016$; Spearman $\rho = 0.92$, $p = 0.0005$), indicating that the groups with higher NF-κB transcription also express the same in P38 MAPK protein expression. This result expresses the functional interconnection and coordinated regulation between the two pathways [9].

Group	NF-κB (RQ, 2−ΔΔCt)	Regulation – NF-κB	p38 MAPK (%)	Regulation – p38 MAPK
G1	1.000	Baseline (normal control)	24.5 ± 0.8	Baseline
G2	2.323	↑ Upregulated (disease control)	33.8 ± 1.4	↑ Upregulated
G3	0.026	↓ Strongly downregulated (30CH)	17.2 ± 2.1	↓ Strongly downregulated
G4	0.253	↓ Downregulated (200CH)	20.2 ± 1.0	↓ Downregulated
G5	0.392	↓ Downregulated (1M)	23.0 ± 0.8	Slightly reduced
G6	0.097	↓ Strongly downregulated (10M)	18.1 ± 0.7	↓ Strongly downregulated
G7	0.349	↓ Downregulated (0/1 LM)	20.8 ± 0.5	↓ Downregulated
G8	0.367	↓ Downregulated (therapeutic, 200CH)	26.1 ± 0.8	Mildly elevated
G9	0.626	↓ Mildly downregulated (Cystone)	27.3 ± 0.9	Mildly elevated

Table 6: *Relative expression of both NF-κB and p38 MAPK in all the groups compared with the normal control*

DISCUSSION

The expressions that were taken for the study of NF-κB transcription and p38 MAPK protein in rat renal tissues treated with ultra- high diluted Berberis vulgaris in the ethylene glycol-induced nephrolithiasis model, both central markers occupy in inflammatory and stress signalling [1–8], so their measurement of renal inflammatory tone, and the strong correlation observed between them ($r = 0.88$, $p = 0.0016$) supports treating the two as a coordinated signalling axis in this dataset [9].

In this study, all the inflammatory-mediated signalling pathways of NF-κB-driven and p38 MAPK induced by ethylene glycol are expressed in the diseased group (G2), showing the highest. G1 is considered the baseline, showing the normal control; the comparison with the disease has marked up-regulation as (2,323- fold) and (33.8 ± 1.4%), respectively. The Berberis vulgaris treated groups has most reduction among two groups occurred at 30CH(G3) and 10M (G6) as (G3: NF-κB 0.026-fold, p38 MAPK 17.2 ± 2.1%; G6: NF-κB 0.097-fold, p38 MAPK 18.1 ± 0.7%), moderate down regulation in G4 (200CH) and G7 (0/1 LM), and G5 (1M), the therapeutic group (G8, 200CH) has slight reduction and standard drug control shows (G9, Cystone) mild elevation compared t the base line. Comparatively, β-actin expression across groups confirmed equal protein loading uniformly.

So, the study shows that there is a consistent report for the anti- inflammatory effect of Berberis Vulgaris [10–12], even though these molecules are not expected to remain in the ultra-dilutions. The study shows NF-κB/p38 MAPK modulation in renal injury models, with an explicit statement of the proposed biological significance for renal inflammation.

LIMITATIONS

- A unsuccussed vehicle-only in control group G1, G2 as a toxic group and G9 cystone as the standard drug of control were not included in the dosing of Berberis vulgaris dilution. So, this method limits the ability to attribute the observed reductions specifically to the ultra-dilution rather than the vehicle or handling effects.
- Densitometry graph expressed in a single plot per group derives the biological replicates blot of the P38 MAPK, strengthening the confidence in the reported differences
- Total p38 MAPK recognises the antibody used (cat. No: 8690) that phosphorylates the activated fraction. Because the functionally activated antibody Phospho- specific should be included in future study
- The complimentary mediators like TNF-α, IL-6, or the phospho/total p38 ratio to assessed with relative narrow marker. This would strengthen the interpretation of the mechanisms
- The exact p- values of the treated group vs disease control vs normal control for full pairwise post-hoc comparisons are reported in the supplementary table, but only the two comparisons in the main text are significant
- The mechanistic basis of any ultra-dilution effect remains unresolved and, as with all high-dilution research, requires blinded, vehicle-controlled, replicated confirmation, ideally with a dilution–response series, before therapeutic conclusions can be drawn.

CONCLUSION

Within these limitations of the present study, ultra-diluted Berberis vulgaris was associated with a marked Upregulation of the NF-kB gene expression in the disease control group, whereas the treated group showed potency and group-dependent downregulation of NF-kB expression, is observed strongest in selected treatment groups. A similar pattern was observed in p38MAPK expression in the diseased – control group and was reduced in treatment with the selected ultra- diluted Berberis Vulgaris. There was a parallel reduction in NF-kB and p38 MAPK expressions, suggesting that the inflammatory signals were reduced in the ethylene glycol nephrolithiasis model. However, these findings should be considered as hypothesis-generating rather than confirmatory, particularly in the absence of comprehensive biological replication and validation. Further studies incorporating adequate biological replicates, a succussed-vehicle control, appropriate blinding, and loading-control-normalised western blot densitometry and statistical comparisons are required to establish the reproducibility and mechanistic significance of these observations.

DECLARATIONS

Ethics approval and consent to participate. All procedures were approved by the Institutional Animal Ethics Committee of Cape Bio Lab and Research Centre, Marthandam, Kanniyakumari District (approval number CBLRC/CLR/47/2022, dated 26 April 2022), in accordance with CPCSEA guidelines, and are reported in line with the ARRIVE 2.0 guidelines.

Consent for publication. Not applicable.

Availability of data and materials. The datasets generated and/or analysed during the current study — raw Ct values, uncropped Western blot images, and ImageJ densitometry files — are available from the corresponding author on reasonable request. [Corresponding author to confirm the specific archive/repository, if any, before submission.]

Competing interests. The authors declare no competing interests.

Funding. Self-funded; no external funding was received.

Authors' contributions:

Dr J. Sundareshan: concepting, methodisation, funding, animal handling and experimentation, formulation of ultra-diluted Berberis Vulgaris, investigations (RNA extraction, qRT-PCR for NF-κB, Western blotting for p38 MAPK), project administration, writing and reviewing the project.

Dr Winston Vargeese: project guidance, data analysis, laboratory guidance, Formal analysis, Software, visualisation, and writing and drafting the data.

Acknowledgements. The authors thank Cape Bio Lab and Research Centre, Marthandam, Kanniyakumari District, Tamil Nadu, India, and Trichy Research Institute of Biotechnology Pvt Ltd, Trichy, Tamil Nadu, India, for laboratory support.

REFERENCES

1. Hayden MS, Ghosh S. NF-κB in immunobiology. Cell Res. 2011;21(2):223–244.
2. Liu T, Zhang L, Joo D, Sun SC. NF-κB signalling in inflammation. Signal Transduct Target Ther. 2017;2:17023.
3. Lawrence T. The nuclear factor NF-κB pathway in inflammation. Cold Spring Harb Perspect Biol. 2009;1(6):a001651.
4. Brasier AR. The NF-κB regulatory network. Cardiovasc Toxicol. 2006;6(2):111–130.
5. Cuenda A, Rousseau S. p38 MAP kinase pathway regulation, function and role in human diseases. Biochim Biophys Acta. 2007;1773(8):1358–1375.
6. Zarubin T, Han J. Activation and signalling of the p38 MAP kinase pathway. Cell Res. 2005;15(1):11–18.
7. Kyriakis JM, Avruch J. Mammalian MAPK signal transduction pathways activated by stress and inflammation. Physiol Rev. 2001;81(2):807–869.

8. Pearson G, Robinson F, Beers Gibson T, Xu BE, Karandikar M, Berman K, et al. Mitogen-activated protein kinase pathways: regulation and physiological functions. Endocr Rev. 2001;22(2):153–183.
9. Perkins ND. Integrating cell-signalling pathways with NF-κB and IKK function. Nat Rev Mol Cell Biol. 2007;8(1):49–62.
10. Imenshahidi M, Hosseinzadeh H. Berberis vulgaris and berberine: an update review. Phytother Res. 2016;30(11):1745–1764.
11. Tillhon M, Guamán Ortiz LM, Lombardi P, Scovassi AI. Berberine: new perspectives for old remedies. Biochem Pharmacol. 2012;84(10):1260–1267.
12. Neag MA, Mocan A, Echeverría J, Pop RM, Bocsan CI, Crişan G, et al. Berberine: botanical occurrence, traditional uses, extraction methods and relevance in cardiovascular, metabolic, hepatic and renal disorders. Front Pharmacol. 2018;9:557.
13. Blackshaw JK, Fenwick DC, Beattie AW, Allan DJ. The behaviour of chickens, mice and rats during euthanasia with chloroform, carbon dioxide and ether. Lab Anim. 1988;22(1):67–75.
14. Hackbarth H, Küppers N, Bohnet W. Euthanasia of rats with carbon dioxide: animal welfare aspects. Lab Anim. 2000;34(1):91–96.
15. Bustin SA, Benes V, Garson JA, Hellemans J, Huggett J, Kubista M, et al. The MIQE guidelines: minimum information for publication of quantitative real-time PCR experiments. Clin Chem. 2009;55(4):611–622.
16. Livak KJ, Schmittgen TD. Analysis of relative gene expression data using real-time quantitative PCR and the 2−ΔΔCT method. Methods. 2001;25(4):402–408.
17. Laemmli UK. Cleavage of structural proteins during the assembly of the head of bacteriophage T4. Nature. 1970;227(5259):680–685.
18. Towbin H, Staehelin T, Gordon J. Electrophoretic transfer of proteins from polyacrylamide gels to nitrocellulose sheets. Proc Natl Acad Sci USA. 1979;76(9):4350–4354.
19. Mahmood T, Yang PC. Western blot: technique, theory, and troubleshooting. N Am J Med Sci. 2012;4(9):429–434.
20. Calabrese EJ, Baldwin LA. Hormesis: the dose-response revolution. Annu Rev Pharmacol Toxicol. 2003;43:175–197.
21. Dei A, Bernardini S. Hormetic effects of extremely diluted solutions on gene expression. Homeopathy. 2015;104(2):116–122.
22. Bellavite P, Marzotto M, Olioso D, Moratti E, Conforti A. High-dilution effects revisited. 1. Physicochemical aspects. Homeopathy. 2014;103(1):4–21.
23. Chen Y, Liu H, Chen H. Ethylene glycol induces calcium oxalate crystal deposition in Malpighian tubules: a *Drosophila* model for nephrolithiasis/urolithiasis. Kidney International, 80, 369-377.
24. Ashurst JV, Schaffer DH, Nappe TM. StatPearls [Internet]. StatPearls Publishing; Treasure Island (FL): Feb 6, 2025. Methanol Toxicity.
25. Ng PCY, Long BJ, Davis WT, Sessions DJ, Koyfman A. Toxic alcohol diagnosis and management: an emergency medicine review. Intern Emerg Med. 2018 Apr;13(3):375-383
26. Beauchamp GA, Valento M. Toxic Alcohol Ingestion: Prompt Recognition And Management In The Emergency Department. Emerg Med Pract. 2016 Sep;18(9):1-20.
27. Kraut JA, Mullins ME. Toxic Alcohols. N Engl J Med. 2018 Jan 18;378(3):270-280.
28. Jacobsen D, McMartin KE. Methanol and ethylene glycol poisonings. Mechanism of toxicity, clinical course, diagnosis and treatment. Med Toxicol. 1986 Sep-Oct;1(5):309-34. Doi: 10.1007/BF03259846. PMID: 3537623.
29. BERMAN LB, SCHREINER GE, FEYS J. The nephrotoxic lesion of ethylene glycol. Ann Intern Med. 1957 Mar;46(3):611-9. doi: 10.7326/0003-4819-46-3-611. PMID: 13403542.